

Enhanced excitonic effects in the energy loss spectra of LiF and Ar at large momentum transfer

S. Sharma^{1,*}, J. K. Dewhurst¹, A. Sanna¹, A. Rubio², and E. K. U. Gross¹

¹ *Max-Planck-Institut für Mikrostrukturphysik, Weinberg 2, D-06120 Halle, Germany. and*

² *Nano-Bio Spectroscopy group and ETSF Scientific Development Centre,*

Centro de Física de Materiales CSIC-UPV/EHU-MPC and DIPC,

Universidad del País Vasco UPV/EHU, Avenida de Tolosa 72, E-20018 San Sebastian, Spain

(Dated: November 12, 2018)

It is demonstrated that the bootstrap kernel [1] for finite values of \mathbf{q} crucially depends upon the matrix character of the kernel and gives results of the same good quality as in the $\mathbf{q} \rightarrow 0$ limit. The bootstrap kernel is further used to study the electron loss as well as absorption spectra for Si, LiF and Ar for various values of \mathbf{q} . The results show that the excitonic effects in LiF and Ar are enhanced for values of \mathbf{q} away from the Γ -point. The reason for this enhancement is the interaction between the exciton and high energy inter-band electron-hole transitions. This fact is validated by calculating the absorption spectra under the influence of an external electric field. The electron energy loss spectra is shown to change dramatically as a function of \mathbf{q} .

PACS numbers:

One of the promising routes for tailoring electromagnetic interactions in systems is to make use of excitons– excitonic condensation[2, 3], exciton-plasmon interaction[4, 5] and strong coupling of excitons with other inter-band optical transitions. A lot of applications of excitonic manipulation have found their way into surface physics, nano-structures and nanotubes. Extended solids, however, have not been treated as serious candidates for such effects. This is mainly due to the fact that excitonic effects are in general (but not exclusively) stronger in lower dimensional systems[6].

As for solids, much of the attention of excitonic physics has been focused on the determination of optical absorption spectra (specially in the long wavelength ($q \rightarrow 0$) limit). Determination of optical absorption spectra in this limit requires an accurate description of electron-hole effects, which in turn requires a computationally expensive many-body treatment at the level of the Bethe-Salpeter equation (BSE)[7–14]. Alternatively, this electron-hole physics can also be effectively treated using time-dependent density functional theory (TDDFT)[15]. However, there exist only a few exchange-correlation (xc) kernels within TDDFT which are capable of accurately describing the excitonic effects arising from strong electron-hole interactions; the computationally demanding but accurate nano quanta kernel[16, 17] which is derived from the BSE, the long-range corrected (LRC) kernel[16, 18, 19] which has the form $\alpha/|q|^2$ (with α being a system dependent external parameter) and the recently proposed bootstrap kernel[1]. The main feature which makes these kernels capable of accurately treating the absorption spectra (in $q \rightarrow 0$ limit) is their $1/|q|^2$ dependence[20], a feature necessary to capture the electron-hole physics.

In contrast to this the optical absorption spectra and the electron energy loss spectra (EELS) at finite values of \mathbf{q} (away from the Γ -point), are known to be accurately

treated[21, 22] by the adiabatic local density approximation (ALDA)[23], which does not have the $1/|q|^2$ dependence. This then raises an interesting question about the validity of the kernels which accurately treat the $\mathbf{q} \rightarrow 0$, for finite values of \mathbf{q} .

In the present work, the EELS and absorption spectra for Si, diamond, LiF and Ar are calculated, using the bootstrap kernel[1] implemented within the ELK code[24]. This choice is motivated by the fact that the bootstrap kernel is computationally not demanding and it does not depend upon any system-dependent parameters. For prototypical materials with bound electron-hole pair, LiF and Ar, there exists a strong coupling between exciton with high energy inter-band transitions, which leads to strong excitonic effects away from the Γ -point. This coupling provides a useful handle to manipulate the excitonic physics, since inter-band transitions can easily be modified by changing external parameters like pressure and/or electric field.

The bootstrap xc-kernel within TDDFT for calculating linear response reads:

$$f_{xc}^{\text{boot}}(\mathbf{q}, \omega) = -\frac{\varepsilon^{-1}(\mathbf{q}, \omega = 0)v(\mathbf{q})}{\varepsilon_0^{00}(\mathbf{q}, \omega = 0) - 1} = \frac{\varepsilon^{-1}(\mathbf{q}, \omega = 0)}{\chi_0^{00}(\mathbf{q}, \omega = 0)} \quad (1)$$

where, v is the bare Coulomb potential, χ_0 is the response function of the non-interacting Kohn-Sham system and $\varepsilon_0(\mathbf{q}, \omega) \equiv 1 - v(\mathbf{q})\chi_0(\mathbf{q}, \omega)$ is the dielectric function in the random phase approximation (RPA). All these quantities are matrices in the basis of reciprocal lattice vectors \mathbf{G} . With a view towards studying the excitonic properties of solids for any value of \mathbf{q} , we first show that the bootstrap kernel for finite values of \mathbf{q} leads to accurate results for the absorption spectra as well as the EELS. This is demonstrated in Fig. 1 which compiles results for the dielectric response and EELS of a small bandgap insulator, Si, a medium badgap insulator, diamond, and a large bandgap insulator, LiF. The choice of these materials is

motivated by the abundance of available experimental data and because they have been used as prototypical test cases for the influence of many-body corrections.

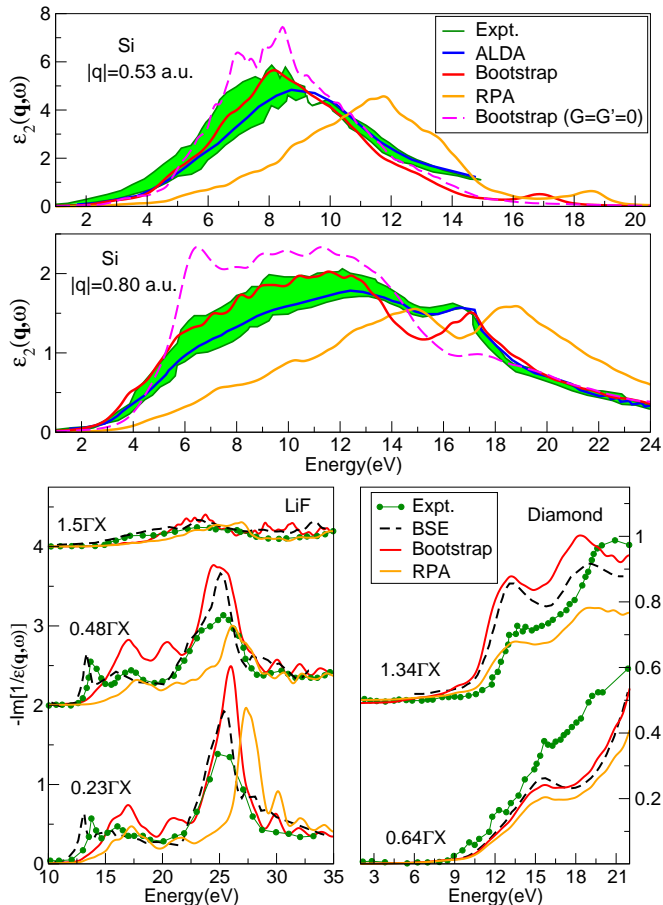


FIG. 1: Upper two panels—imaginary part of the dielectric tensor as a function of energy in eV for Si. Results obtained using the bootstrap kernel, RPA and ALDA are compared with experimental data from Ref. 22. The top panel contains results for $|\mathbf{q}| = 0.53 \text{ a.u.}$ and the middle panel for $|\mathbf{q}| = 0.80 \text{ a.u.}$ parallel to the $[111]$ direction. The bootstrap results are obtained in two different ways; (red line) the kernel is a full matrix in the reciprocal space with $|\mathbf{G}|_{\text{max}} = 4 \text{ a.u.}$ and (pink dotted line) only the head of the kernel is used i.e. $|\mathbf{G}|_{\text{max}} = 0 \text{ a.u.}$ The bottom panel contains results for the EELS, for different values of \mathbf{q} (indicated in the figure) as a function of energy in eV for LiF and diamond. The results obtained using the bootstrap kernel are shown with full line, the experimental data (from Ref. 25) with dots and the BSE results (also taken from Ref. 25) with dashed line. The results for different values of \mathbf{q} are shifted vertically for clarity.

The upper two panels of Fig. 1 are presented the results for $\epsilon(\mathbf{q}, \omega)$ of Si. The results obtained using the bootstrap kernel are compared to the results obtained using the ALDA and to the experimental data. It is clear that as far as the absorption spectrum is concerned the bootstrap kernel (treated as a full matrix in reciprocal space) gives results in good agreement with experiments.

Interestingly, for small frequencies the results obtained using the bootstrap kernel give an upper bound to the experimental data, while the results obtained using the ALDA give a lower bound. The RPA results (also shown in Fig. 1), as expected, totally miss the excitonic physics, which in this case shows up as the shifting of the spectral weight to lower frequencies.

In the $\mathbf{q} \rightarrow 0$ limit the $\mathbf{G} = \mathbf{G}' = 0$ component of f_{xc} is the most important one and hence the bootstrap procedure can be thought of as a self-consistent method for obtaining the system dependent parameter α of the LRC. While, for finite values of \mathbf{q} the matrix character of f_{xc} is crucial and the bootstrap kernel is significantly different from the LRC kernel. The importance of including higher \mathbf{G} vectors in f_{xc} is demonstrated in Fig. 1; results for Si show that the dielectric function obtained using only the $\mathbf{G} = \mathbf{G}' = 0$ component of f_{xc} are much higher in magnitude and in relatively poor agreement with the experimental data.

EELS corresponds to the negative of the imaginary part of $\epsilon_{00}^{-1}(\mathbf{q}, \omega)$, where 00 stands for the $\mathbf{G} = \mathbf{G}' = 0$ component of the dielectric tensor. The lower panel of Fig. 1 contains results for the EELS of LiF and diamond. Three different values of \mathbf{q} in the $\Gamma - X$ direction are presented for LiF. Within the first BZ the experimental data and BSE results show three main peaks which are well reproduced by the bootstrap kernel. On going from 0.23 to $0.48 \Gamma X$ the plasmonic peak at 25 eV gets smaller in magnitude, a feature which is again well captured by the bootstrap kernel. Experiments, BSE and bootstrap results show that outside the first BZ (for $\mathbf{q} = 1.50\Gamma X$) EELS is highly suppressed. These results indicate that the bootstrap kernel captures the change in $-\text{Im}[\epsilon^{-1}]$ as a function of \mathbf{q} very well. We note, however, that the magnitude of the peaks is slightly overestimated by the bootstrap kernel and, for small energies, the peaks are blue shifted by $\sim 1 \text{ eV}$ compared to experiment. This shifting of the excitonic peaks to higher frequencies and the overestimation of their magnitude was also a feature of the absorption spectra in the long wavelength limit.

For diamond, the magnitude of the EELS obtained using the bootstrap kernel is overestimated compared to the experiment. A similar overestimation is also seen in the BSE results[25]. In fact, we find that the results obtained using the bootstrap kernel are in very good agreement with the BSE results. As in the case of Si, for LiF and diamond as well, the RPA results are shifted to higher frequencies and are missing excitonic physics.

It is apparent from the examples above that the bootstrap results for values of \mathbf{q} away from the Γ -point, have the same good agreement with experiments as those in the $\mathbf{q} \rightarrow 0$ limit. With this in hand we can now use the bootstrap kernel to study the excitonic effects in various directions in the BZ.

In Fig. 2 the results for $\epsilon(\mathbf{q}, \omega)$ are shown for LiF and Ar for various values of \mathbf{q} . The upper panel con-

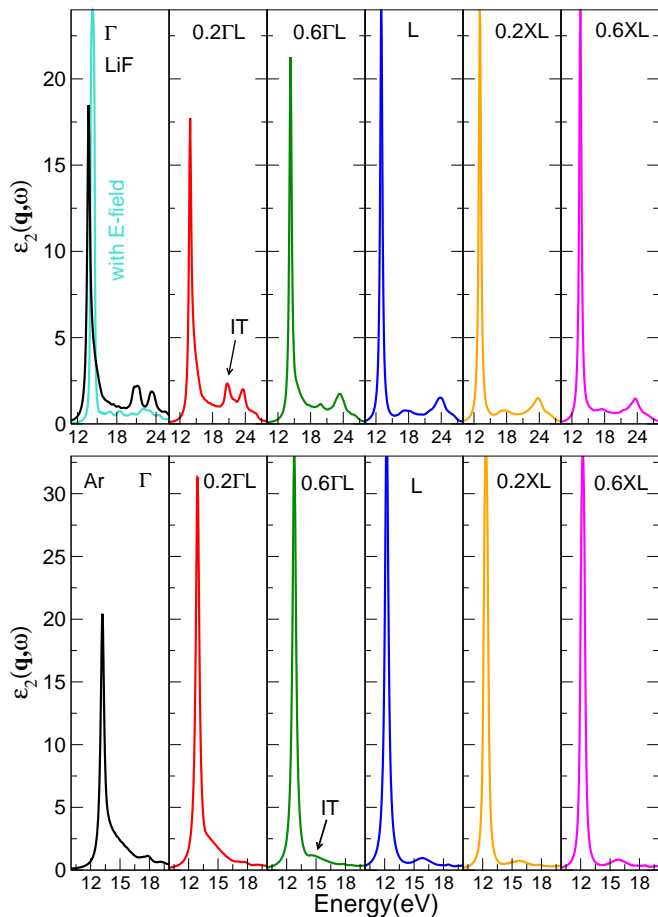


FIG. 2: Dielectric tensor obtained using the bootstrap kernel as a function of energy in eV. Upper panel contains results for LiF and the Lower panel for Ar in the $\Gamma - L - X$ direction. The upper-left most panel also contains results at the Γ -point for LiF exposed to an external electric field.

tains results for LiF in the $\Gamma - L - X$ direction[26]. It is immediately clear from this that the excitonic peak in LiF becomes stronger (spectral weight moves to lower frequency) away from the Γ -point; on going from Γ to L , the excitonic peak (~ 13 - 14 eV) becomes larger in magnitude and at the same time the inter-band transition (IT) peak ~ 20 eV diminishes and moves to lower frequencies (from 20 eV to 18 eV). In the $L - X$ direction the excitonic and IT peaks remain almost the same.

Similar results are also seen for Ar; on going from Γ to L , the spectral weight moves towards the excitonic peak (~ 12 eV) which becomes stronger and shifts to lower frequencies. This is accompanied by a steady diminishing of the IT peak around 18 eV. Beyond $0.6\Gamma L$, both the excitonic and the IT peaks are unchanged. The RPA for both LiF and Ar misses this excitonic physics for all values of \mathbf{q} .

The above results point towards a strong coupling between the excitonic and the IT peaks; as the excitonic peak gains weight, the IT peak diminishes. This obser-

vation could be used in the future to tune excitonic effects via manipulation of inter-band transitions. In order to validate this hypothesis we have performed calculations of the $\mathbf{q} \rightarrow 0$ absorption spectrum for LiF in presence of an external electric field. This field is an artifice used to lift the degeneracy and split the bands. This split in the bands causes the IT peak at 20 eV to diminish and move to lower energies. The excitonic peak gains weight (spectral weight moves to lower energy) and the results for ε in the $\mathbf{q} \rightarrow 0$ limit closely resemble those of the L -point (see top-first panel of Fig. 2). Such a tuning of the excitons has been performed before: a coupling of excitons and surface plasmons was used to enhance excitonic effects in low dimensional systems[4, 5, 27].

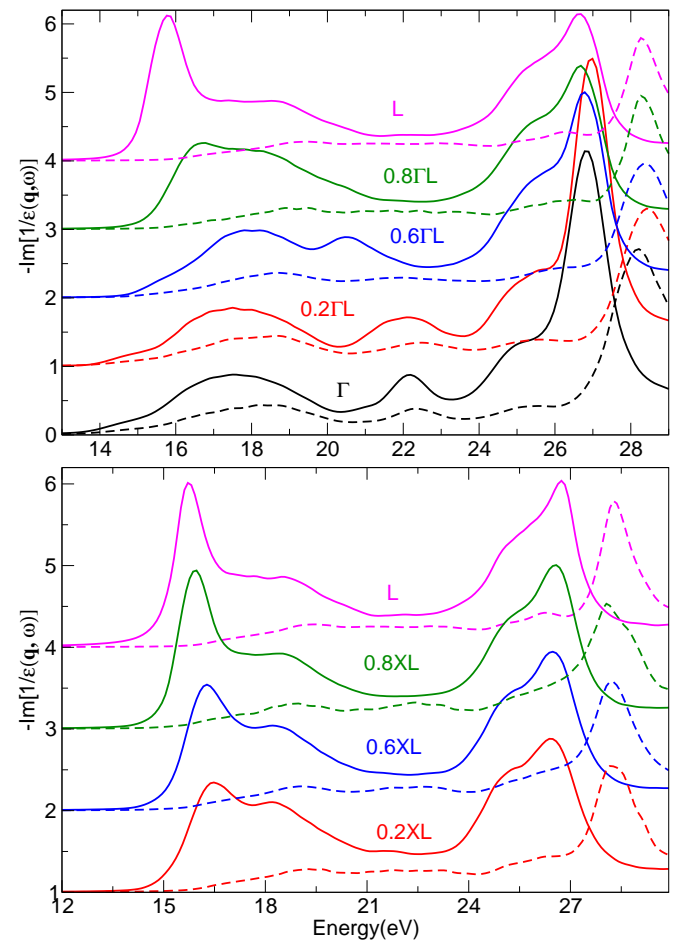


FIG. 3: Electron energy loss spectrum ($-Im[\varepsilon_{00}^{-1}(\mathbf{q}, \omega)]$) in arbitrary units as a function of energy in eV for LiF. Results obtained using the bootstrap kernel are shown with full lines and the results obtained using the RPA are shown with dashed lines. Upper panel shows results in the $\Gamma - L$ direction and lower panel in the $X - L$ direction. Results for various values of \mathbf{q} are shifted vertically for clarity.

$\varepsilon_{00}^{-1}(\mathbf{q}, \omega)$ is an important quantity, not just because it can be directly compared to experiments, but also because it is required for an accurate determination of the

screened Coulomb interaction, $W = \varepsilon^{-1}v$. In Hedin's theoretical foundation of many-body perturbation theory the effective interaction, W , is a crucial concept. It is needed as an essential ingredient if one wishes to sum Feynman diagrams to obtain the Green's function of a system[7, 9]. In Fig. 3 we present results for the EELS of LiF as a function of \mathbf{q} and frequency. The EELS changes dramatically as a function of \mathbf{q} ; the peak at 16 eV gains height on moving in the $\Gamma - L$ direction (upper panel), while at the same time the peak at 25 eV diminishes in magnitude and broadens. This leads to the EELS for $\mathbf{q} \rightarrow 0$ being significantly different from that at $\mathbf{q} = [0.5, 0.5, 0.5]$. A similar sharpening of the peak at 16 eV is also seen in the $L - X$ direction (lower panel); A broad double peak at ~ 18 eV changes to one sharp peak at 16 eV and a small shoulder at ~ 20 eV. In the $L - X$ direction (unlike the $\Gamma - L$) the peak at 25 eV stays almost unchanged as a function of \mathbf{q} . Similar strong changes in EELS as a function of \mathbf{q} , in the $\Gamma - U$ direction for LiF, have been reported before in Ref. [28].

The RPA results (also shown in Fig. 3) not only miss the low energy excitonic effects[28], but also show very little variation as a function of \mathbf{q} in both the $\Gamma - L$ and $X - L$ directions. Most many-body calculations use RPA dielectric functions for screening the Coulomb potential. However, it is clear from the present study that RPA dielectric functions can wildly differ from those which properly include electron-hole physics. TDDFT with the bootstrap kernel is a computationally efficient method to accurately determine $\varepsilon^{-1}(\mathbf{q}, \omega)$ for use in many-body perturbation theory[28].

To summarize, in the present work it is demonstrated that results obtained using the bootstrap kernel for finite values of \mathbf{q} have the same accuracy as those in the $\mathbf{q} \rightarrow 0$ limit. We use this kernel to make the predictions that in the prototypical materials LiF and Ar excitonic effects are enhanced *away* from Γ . The reason for this enhancement is attributed to the interaction between the exciton and other high energy inter-band transitions. This observation is reinforced by the application of an external electric field and noting an inverse proportionality in strengths between the inter-band and excitonic peaks. It is further demonstrated that the EELS also changes dramatically as a function of \mathbf{q} . This strong change in EELS is missing within the RPA, and hence it is highly desirable to use a TDDFT dielectric function to screen the Coulomb interaction as input for many-body perturbation theory.

AR acknowledges funding from European Research

Council Advanced Grant DYnAmo (ERC-2010-AdG - Proposal No. 267374), Spain (FIS2010-21282-C02-01 and PIB2010US-00652), Grupos Consolidados UPV/EHU del Gobierno Vasco (IT-319-07) and ACI-Promociona (ACI2009-1036).

* Electronic address: sharma@mpi-halle.mpg.de

- [1] S. Sharma, J. K. Dewhurst, A. Sanna, and E. K. U. Gross, Phys. Rev. Lett. **107**, 186401 (2011).
- [2] L. V. Keldysh and Y. V. Kopayev, Fiz. Tverd. Tela **6**, 2781 (1964).
- [3] J. P. Eisenstein and A. H. MacDonald, Nature **432**, 691 (2004).
- [4] I. V. Bondarev, L. M. Woods, and K. Tatur, Phys. Rev. B **80**, 085407 (2009).
- [5] J. Bellessa, C. Bonnand, J. C. Plenet, and J. Mugnier, Phys. Rev. Lett. **93**, 036404 (2004).
- [6] L. Wirtz, A. Marini, and A. Rubio, Phys. Rev. Lett. **96**, 126104 (2006).
- [7] W. Hanke, Adv. Phys. **27**, 278 (1978).
- [8] G. Onida *et al.*, Phys. Rev. Lett. **75**, 818 (1995).
- [9] G. Onida *et al.*, Rev. Mod. Phys. **74**, 601 (2002).
- [10] M. Rohlfing and S. G. Louie, Phys. Rev. Lett. **81**, 2312 (1998).
- [11] R. Laskowski and N. E. Christensen, Phys. Stat. Sol. (b) **244**, 17 (2007).
- [12] P. H. Hahn *et al.*, Phys. Stat. Sol. (b) **242**, 2720 (2005).
- [13] F. Bechstedt *et al.*, Phys. Rev. B **72**, 245114 (2005).
- [14] S. Galamic-Mulaomerovic and C. H. Patterson, Phys. Rev. B **72**, 035127 (2005).
- [15] E. Runge and E. K. U. Gross, Phys. Rev. Lett. **52**, 997 (1984).
- [16] L. Reining *et al.*, Phys. Rev. Lett. **88**, 066404 (2002).
- [17] A. Marini, R. Del Sole, and A. Rubio, Phys. Rev. Lett. **91**, 256402 (2003).
- [18] S. Botti *et al.*, Phys. Rev. B **69**, 155112 (2004).
- [19] S. Botti *et al.*, Phys. Rev. B **72**, 125203 (2005).
- [20] P. Ghosez *et al.*, Phys. Rev. B **56**, 12811 (1997).
- [21] S. Botti *et al.*, Rep. Prog. Phys. **70**, 357 (2007).
- [22] H.-C. Weissker, J. Serrano, S. Huotari, E. Luppi, M. Cazzaniga, F. Bruneval, F. Sottile, G. Monaco, V. Olevano, and L. Reining, Phys. Rev. B **81**, 085104 (2010).
- [23] E. K. U. Gross, F. J. Dobson, and M. Petersilka, Topics in Current Chemistry **181**, 81, (1996) (and references therein).
- [24] (2004), URL <http://elk.sourceforge.net>.
- [25] W. A. Caliebe, J. A. Soininen, E. L. Shirley, C.-C. Kao, and K. Hämäläinen, Phys. Rev. Lett. **84**, 3907 (2000).
- [26] $\Gamma - L - X = [0, 0, 0] - [0.5, 0.5, 0.5] - [0.5, 0.5, 0]$.
- [27] C. Attaccalite, M. Bockstedte, A. Marini, A. Rubio, and L. Wirtz, Phys. Rev. B **83**, 144115 (2011).
- [28] A. Marini and A. Rubio, Phys. Rev. B **70**, 081103 (2004).